Quench Performance of a 4-m Long Nb_3Sn Shell-type Dipole Coil

G. Chlachidze, G. Ambrosio, N. Andreev, E. Barzi, R. Bossert, R. Carcagno, V.S. Kashikhin, V.V. Kashikhin, M.J. Lamm, F. Nobrega, I. Novitski, D. Orris, C. Sylvester, M. Tartaglia, J.C. Tompkins, D. Turrioni, G. Velev, R. Yamada, A.V. Zlobin

***Abstract*— Fermilab has finished the first phase of Nb_3Sn technology scale up by testing 2-m and 4-m long shell-type dipole coils in a 'magnetic mirror' configuration. The 2-m long coil, made of Powder-in-Tube (PIT) Nb_3Sn strand, reached its short sample limit at a field level of 10 T. The 4-m long coil, made of advanced Nb_3Sn strand based on the Restack Rod Process (RRP) of 108/127 design, has been recently fabricated and tested. Coil test results at 4.5 K and 2.2 K are reported and discussed.**

***Index Terms*— accelerator magnets, Nb_3Sn strand, cable, coil, dipole mirror, superconducting magnet, quench, stability.**

I. Introduction

FERMILAB is developing a new generation of accelerator magnets based on Nb_3Sn superconductor and wind-and-react technology. After testing of several 1-m long dipole coils, a Nb_3Sn technology scale-up program has been launched with the goal to expand the developed Nb_3Sn coil technology to long coils and to prepare fabrication and test infrastructure [1]. The first phase of this program has been accomplished by fabricating and testing 2-m and 4-m long shell-type Nb_3Sn dipole coils. This phase has addressed some key scale up issues including the long Nb_3Sn coil winding, curing, reaction, impregnation, and handling, as well as long Nb_3Sn magnet assembly and long coil performance.

The 2-m long coil was made of PIT Nb_3Sn strand which has demonstrated good stability and reproducible performance [2]. The 4-m long coil was made of advanced RRP Nb_3Sn strand. Prior to making the long Nb_3Sn coils, one practice coil of each length was made using copper cable to test the tooling and verify key steps in the process. Both long Nb_3Sn coils were tested in a magnetic 'mirror' configuration based on the dipole mechanical structure [3]. The mirror model with a 2-m long PIT coil reached its conductor limit and reproduced the quench performance of the 1-m long reference coil [4],[5]. This paper summarizes the fabrication and test results of the first 4-m long Nb_3Sn shell-type coil based on the RRP strand.

Manuscript received August 26, 2008. Work supported by Fermi Research Alliance, LLC under contract No. DE-AC02-07CH11359 with the U.S. Department of Energy.

Authors are with the Fermi National Accelerator Laboratory (Fermilab), P.O. Box 500, Batavia, IL 60510 USA (phone: 630-840-4622; fax: 630-840-8079; e-mail: guram@fnal.gov).

II. Coil Design and Fabrication

A. Coil and Cable Parameters

The coil has 2-layer shell-type cross-section, with 16 turns and two spacers per quadrant in the inner layer, 21 turns and two spacers per quadrant in the outer layer, and pole blocks in each layer. Coil layers are separated by 0.4 mm thick inter-layer insulation. The end current blocks, separated by end spacers, match the coil straight section. The pole blocks and spacers are made of aluminum bronze.

The coil design is based on Rutherford cable with 27 1-mm diameter strands. RRP strand of a 108/127 stack cross-section was produced by Oxford Superconductor Technologies, Inc. [6]. The 1-mm RRP strand of this design has a sub-element size of ~70 μm, a copper fraction of 49% and a twist pitch of 12 mm, providing a nominal J_c of ~2400 A/mm^2 at 4.2 K and 12 T with a Cu-matrix residual resistivity ratio above 200 [7].

B. Coil Fabrication and Mirror Assembly

The details of the long Nb_3Sn coil fabrication procedure are described in [5]. The 4-m long coil was wound from a single ~180-m long piece of cable without an inter-layer splice. The cable insulation consisted of two layers: the first layer was made of 75 μm thick E-glass tape with a 50% overlap and the second layer was made with a butt lap of 75 μm thick S2-glass tape.

The coil was reacted in a 3-step cycle with the last step at 646^{o}C for 51 hours and then impregnated with CTD 101K epoxy. A picture of the coil after reaction is shown in Fig. 1. The coil dimensions were measured in the free state after impregnation to select appropriate pre-stress shims. Flexible NbTi leads were soldered to each of the inner and outer Nb_3Sn leads. Voltage taps were placed across each coil block to detect and localize quenches.

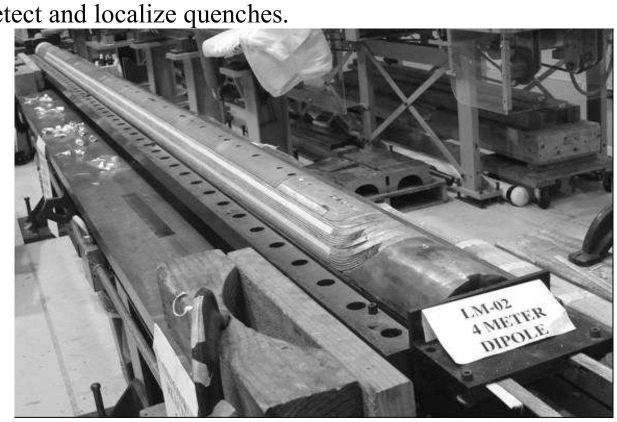

Fig. 1. 4-m long Nb_3Sn RRP coil.

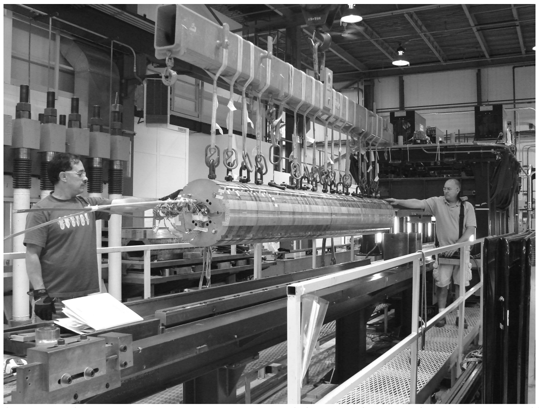

Fig. 2. Mirror LM02 (HFDM08) with 4-m long Nb_3Sn RRP coil.

The coil was tested in dipole ‘mirror’ configuration [3]. The mirror mechanical structure is similar to the normal dipole structure except that one of the two coils is replaced by half-cylinder blocks made of solid iron. Mirror magnet LM02 (HFDM08) with a 4-m long Nb_3Sn RRP coil is shown in Fig.2. Transverse preload to the coil was applied by a combination of the aluminum yoke clamps and the 8-mm thick welded stainless steel skin. Axial support was provided through end bolts attached to the end plates. The coil azimuthal stress was determined from capacitive and resistive strain gauge measurements. The axial coil preload was set using measurements from resistive strain gauges on the bolts.

The target coil pre-stress at room temperature was determined based on ANSYS analysis with elasto-plastic coil properties [8]. The nominal maximum coil pre-stress was ~80 MPa. The strain gauge data confirmed that the target coil pre-stress during assembly has been achieved.

III. Test Results

LM02 (HFDM08) was tested in boiling liquid helium at 4.5 K and at lower temperatures in two thermal cycles.

A. Initial Quench Performance

The first 65 quenches are presented in Fig. 3. At 4.5 K, the magnet training started with quenches in low field region of the outer layer (mid-plane block). The magnet performance was rather erratic with quench currents varying from ~15 kA to ~17 kA without any training.

At ramp rates of 150 A/s and higher, the magnet quenched at 3-4 kA with quenches originating in the mid-plane blocks of both the inner and outer coil layers. It was found empirically that much higher quench currents were reached at the same high ramp rates if “conditioning” ramps were used prior to the ramp to quench. During “conditioning”, the current was ramped up to ~10 kA and then down to 0 A, both at the rate of 100 A/s. Subsequently it was found that the quenches in the 3-4 kA region are avoided if the magnet is first ramped to 5 kA at a low ramp rate and then ramped to quench at high ramp rates. Conditioning ramps nevertheless did not improve the quench performance at low ramp rates and the magnet still quenched at the same current in the outer layer.

Following the ramp rate study at 4.5 K, the magnet was cooled to 2.2 K. However, the magnet performance did not change. In fact, no temperature dependence was observed at low or high ramp rates.

Erratic quench performance at currents far from the expected conductor limit (23.7 kA at 4.5 K and 26.0 kA at 2.2 K based on the short sample data), without any sign of training or temperature dependence, is consistent with the magnetic instability previously observed in short dipole and mirror models [9]. In the reference short coil made of the same cable the flux jumps were also observed but at the higher current level of ~21 kA [10].

B. Flux Jump Suppression Using Quench Heater

To suppress the flux-jump instabilities in the coil, a quench protection strip heater conveniently located on the outer coil surface next to the mid-plane block was used to “warm” the coil.

An extensive thermal analysis was performed using the *COMSOL Multiphysics* code in order to estimate the temperature in different coil segments, as well as the total power dissipation as a function of the heater power. A typical temperature distribution in the coil cross-section produced by the strip heater on the mid-plane block is shown in Fig. 4. With the heater on, the peak coil temperature occurs in the outer mid-plane block. At a certain level of the heater power the inner mid-plane block has the lowest quench margin due to the higher field in the inner layer.

During the test the heater current varied within 2-3 A range corresponding to the total dissipated power from 40 to 100 W.

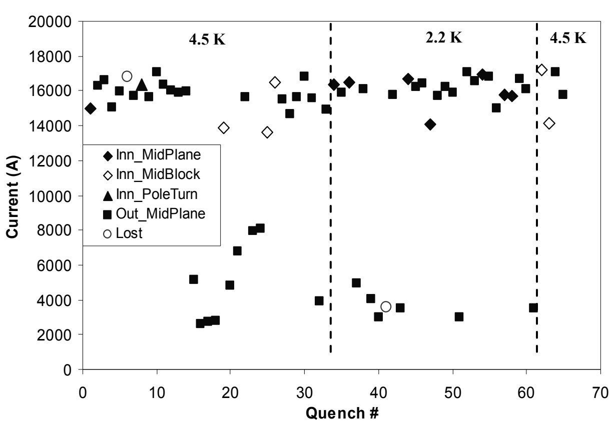

Fig. 3. Detailed quench locations for the first 65 quenches.

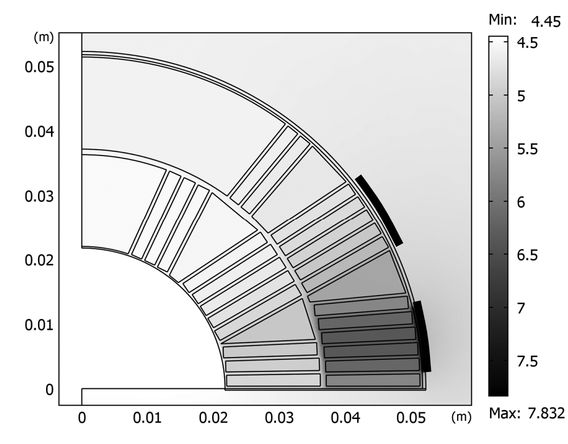

Fig. 4. Temperature distribution in the coil cross-section with the mid-plane heater on. The locations of the two strip heaters are indicated.

The maximum heat flux was 220 W/m^2 for the middle turn of the inner-layer mid-plane block, which is at least an order of magnitude lower than the helium film-boiling threshold. Consequently, no heat-related problems were observed in the cryogenic system during the test.

C. Quench Performance with Suppressed Instabilities

Testing with the heater began after quench #66 when the magnet was warmed up to 4.5 K. The first three quenches at a 2.02 A heater current still occurred in the outer layer, but now the magnet did not exhibit the erratic behavior and started quenching at almost the same current. The first training quench occurred in the pole blocks of the inner layer at a heater current of 2.55 A. Later on it was shown that instability in the outer layer is quite sensitive to the heater power and to the amount of heat transferred from the heater to the coil, i.e. to the coil temperature.

At the end of first thermal cycle (TC-1) it was demonstrated that much higher quench currents were reached with the heater current on (i.e. with a "warmed" mid-plane block in the outer layer). In quench #102, the heater was switched off and the magnet quenched again in the outer-layer mid-plane block at a significantly lower current (see Fig. 5). The highest quench current reached in the 1st thermal cycle ~20.1 kA was quench #104 at a ramp rate of 5 A/s and a heater current of 2.38 A. With quench #106, TC-1 was completed and the magnet was warmed to room temperature.

The second thermal cycle (TC-2) started with quench #107 at a current of ~16 kA with the strip heater off. The quench current and location was consistent with quenches at the beginning of TC-1. Then the heater was switched on and the magnet showed some training with quenches in the pole block of the inner layer. In quench #112, a current of ~19.7 kA was reached with a strip heater current of 2.38 A.

After quench #115, the magnet was cooled to 2.2 K to perform heater tests at lower temperature. After a short training period with a heater current of 3.05 A the magnet quench current increased to 20.2-20.4 kA. The testing at 2.2 K was finished with a ramp rate study and the highest quench current of ~20.6 kA was reached in quench #135 at a ramp rate of 10 A/s.

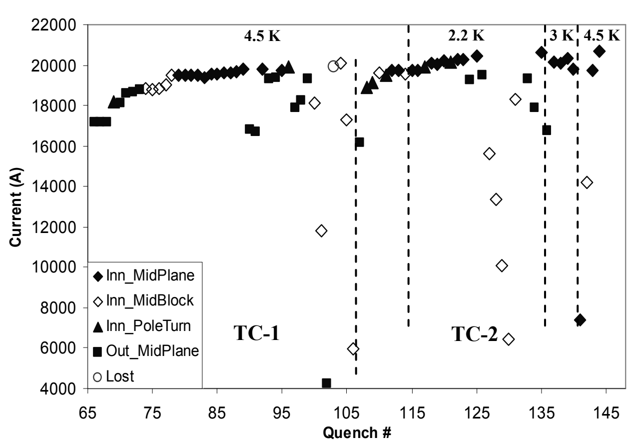

Fig. 5. Quench locations with the strip heater on. The heater current was switched off for quenches #102 and #107.

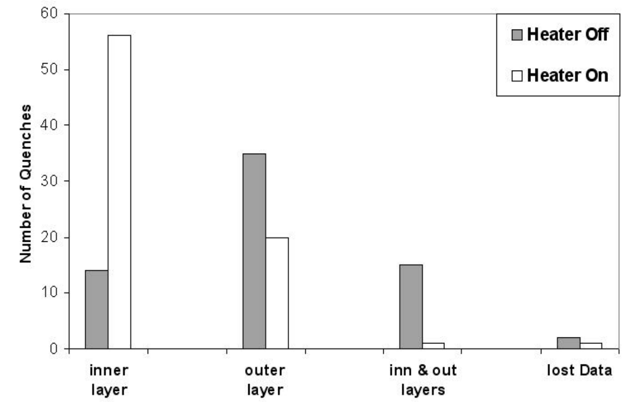

Fig. 6. Quench multiplicity in the inner and outer layers with and without current on the streap heater.

At 3.1K, the magnet was quenched 5 times with the strip heater on to study the temperature dependence of the quench performance. The quench program in TC-2 was completed at 4.5 K by taking few more quenches at different ramp rates. The heater current was set to 2.39 A as it was during the ramp rate study at 4.5 K in the first thermal cycle.

At the very end of TC-2 the magnet was ramped up to ~ 19 kA at the rate of 10 A/s, then the heater current was reduced from 2.39 A to 0 A, lowering the temperature of the inner layer mid-plane block. In this case the quench current increased to 20.7 kA which is 87.4% of the estimated short sample limit for the magnet at 4.5 K. This was the maximum current reached during the testing of this magnet.

Quench multiplicity in the inner and outer layers, with and without the strip heater, is summarized in Fig. 6. In total, 144 quenches were performed, and in only 8 cases a quench developed in the inner-layer pole block. The estimated locations for these 8 quenches are in the innermost turn and they were not concentrated in a particular region.

D. Ramp Rate Dependence

Several quenches were performed for the ramp rate dependence study at 4.5 K and 2.2 K in both thermal cycles. The ramp rate dependence for quenches in the inner layer only (i.e. with the strip heater on) is shown in Fig. 7.

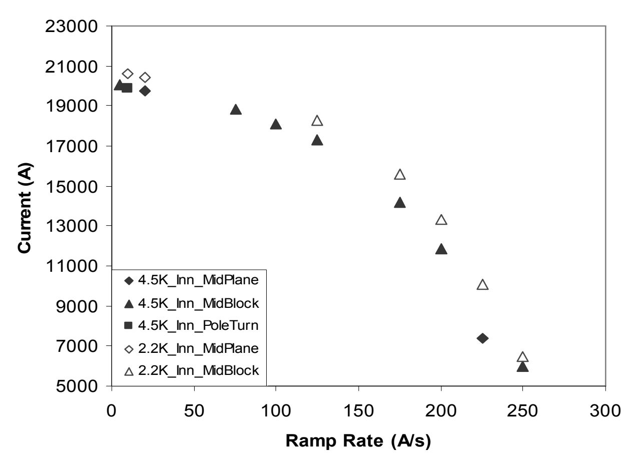

Fig. 7. LM02 (HFDM08) ramp rate dependence (inner layer quenches only).

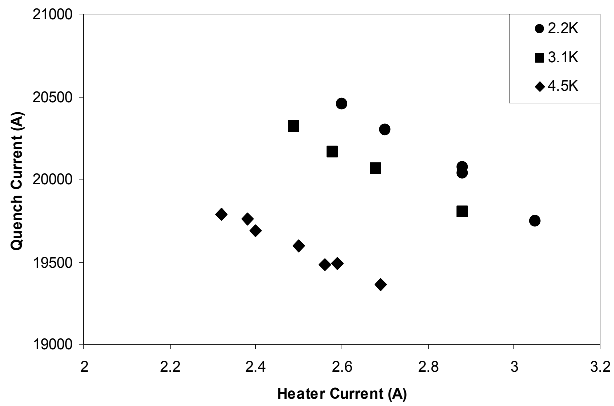

Fig. 8. Quench current vs. heater current for the inner-layer mid-plane block.

One can see that the quench current decreases with increasing current ramp rate or temperature. The shape of this ramp rate dependence is consistent with measurements on the reference short model HFDM06 [10]. However, the maximum quench current of the magnet in the highest field region (the inner-layer pole block) cannot be extrapolated from this dependence since only one quench occurred in the pole block during the ramp rate study.

E. Temperature Dependence

Quenches originating only in the inner-layer mid-plane blocks for three different test temperatures 4.5 K, 3.1 K and 2.2 K at a ramp rate of 20 A/s are plotted in Fig. 8. This plot illustrates that the measurements at different temperatures are consistent and clearly exhibit similar temperature dependence.

A parabolic extrapolation of data in Fig. 8 to zero heater power allows the cable critical current in the inner-layer mid-plane block to be estimated. These data are presented in Table I. Calculated critical currents for the inner-layer mid-plane block, based on the magnet short sample limit of 23.7 kA at 4.5 K, as well as the critical current of the inner-layer pole block (which determines the magnet critical current limit), at different temperatures are shown in this table.

Based on the data in Table I, degradation of the cable critical current in the inner-layer mid-plane block reaches ~23%. This degradation could be due to the compressive stress ~100 MPa (according to ANSYS calculations) applied to the cable in the mid-plane block during excitation [11] or due to the non-uniform current distribution in the mid-plane blocks close to the coil leads. The latter could also explain the lower level of instability current in LM02 (HFDM08) with respect to the reference HFDM06 [10].

F. Residual Resistivity Ratio (RRR)

The conductor RRR in LM02 (HFDM08) coil blocks was measured during magnet warm-up between the two thermal cycles. During the cold RRR measurement the temperature of the magnet at top, middle and bottom were 23.7 K, 20.5 K and 17.2 K respectively. The total coil RRR is 158, the inner layer and the outer layer RRR values are 153 and 166 respectively. The measured variations of coil RRR for the reference short model HFDM06 were 172±3 [10].

TABLE I Inner-layer midplane block calculated Ic_calc and extrapolated from the heater study Ic_extr critical currents.

T (K)	Ic_calc (kA)	Ic_extr (kA)	Ic_extr/Ic_calc	Ic_pole (kA)
2.2	29.12	22.291	0.765	26.06
3.1	28.21	21.781	0.772	25.25
4.5	26.5	21.086	0.796	23.7

IV. Conclusions

The first 4-m long shell-type Nb_3Sn coil made of 1-mm RRP strand with 108/127 sub-elements was fabricated and successfully tested at Fermilab in a mirror configuration. Initially the quench current was limited by low-field flux jump instabilities both at 4.5 K and 2.2 K. Significant improvement was achieved by locally heating the outer layer mid-plane block using one of the quench protection heaters. As a result of flux jump suppression, the quench location moved from the outer to the inner-layer mid-plane block.

The maximum quench current reached in this test was 20.7 kA at 4.5 K, which is 87.4% of the estimated short sample limit for the magnet at this temperature. The magnet training was not completed due to limitations related to coil heating by the strip heater. These test results confirm significant progress towards controlled fabrication and successful performance of long Nb_3Sn accelerator magnets. This work complements the Nb_3Sn technology scale up program for LARP in preparation to the fabrication and test of 4-m long large-aperture Nb_3Sn quadrupoles of LQ series [12], [13].

V. Acknowledgements

The authors would like to thank the technical staff at the Fermilab Technical Division for their contribution to the magnet fabrication and test.

References

[1] F. Nobrega et al., “Nb_3Sn accelerator magnet technology scale up based on cos-theta coils”, *IEEE Trans. on Applied Superconductivity*, Volume 17, Issue 2, June 2007 Page(s): 1031-1034.

[2] A.V. Zlobin et al., ”Development and test of Nb_3Sn cos-theta dipoles based on PIT strands”, *IEEE Trans. on Applied Superconductivity*, Volume 15, Issue 2, June 2005 Page(s):1160 – 1163

[3] D.R. Chichili et al., “Design, fabrication and testing of Nb_3Sn shell type coils in mirror magnet configuration”, *CEC/ICMC* 2003, Alaska, September 22-25 2003.

[4] A.V. Zlobin et al., “Development of Nb_3Sn accelerator magnet technology at Fermilab”, *Proceedings of 2007 Particle Accelerator Conference, Albuquerque*, NM, June 2007.

[5] F. Nobrega et al., “Nb_3Sn accelerator magnet technology scale-up using cos-theta dipole coils”, *IEEE Trans. on Applied Superconductivity*, Volume 18, Issue 2, June 2008 Page(s): 273 - 276.

[6] S. Hong et al., “Latest improvements of current carrying capability of niobium tin and its magnet applications”, *IEEE Trans. on Applied Superconductivity*, Vol. 16, Issue 2, 2005, p. 1146.

[7] E. Barzi et al., “Performance of Nb_3Sn RRP strands and cables based on a 108/127 stack design”, *IEEE Trans. on Applied Superconductivity*, Vol. 17, Issue 2, June 2007 Page(s): 2718-2721.

[8] D. R. Chichili, et al., “Investigation of cable insulation and thermo-mechanical properties of epoxy impregnated Nb_3Sn composite”, *IEEE Trans. on Applied Superconductivity*, v. 10, No. 1, March 2000, p.1317.

[9] S. Feher et al., “Test results of Shell-type Nb_3Sn dipole coils”, *IEEE Trans. on Applied Superconductivity*, Vol. 14, Issue 2, June 2004 Page(s): 349 – 352.

[10] A.V. Zlobin et al., “Quench performance of Nb_3Sn cos-theta coil made of 108/127 RRP strands”, *CEC/ICMC* 2007, Chattanooga, TN, July 16-20, 2007.

[11] E. Barzi et al., “Effect of transverse pressure on brittle superconductors”, *IEEE Trans. on Applied Superconductivity*, Volume 18, Issue 2, June 2008 Page(s): 980 - 983

[12] P. Wanderer et al., **“**Construction and test of 3.6 m Nb_3Sn racetrack coils for LARP”, *IEEE Trans. on Applied Superconductivity*, Volume 18, Issue 2, June 2008 Page(s): 171 - 174.

[13] G. Ambrosio et al., “LARP long Nb_3Sn quadrupole design”, *IEEE Trans. on Applied Superconductivity*, Volume 18, Issue 2, June 2008 Page(s): 268 – 272.